Transitions in the Learnability of Global Charges from Local Measurements

Fergus Barratt, ¹ Utkarsh Agrawal, ^{1,2} Andrew C. Potter, ³ Sarang Gopalakrishnan, ^{4,5} and Romain Vasseur ¹ Department of Physics, University of Massachusetts, Amherst, Massachusetts 01003, USA ² Kavli Institute for Theoretical Physics, University of California, Santa Barbara, California, USA ³ Department of Physics and Astronomy, and Quantum Matter Institute, University of British Columbia, Vancouver, British Columbia, Canada V6T 1Z1 ⁴ Department of Physics, The Pennsylvania State University, University Park, Pennsylvania 16802, USA ⁵ Department of Electrical and Computer Engineering, Princeton University, Princeton, New Jersey 08544, USA

(Received 8 July 2022; accepted 18 October 2022; published 10 November 2022)

We consider monitored quantum systems with a global conserved charge, and ask how efficiently an observer ("eavesdropper") can learn the global charge of such systems from local projective measurements. We find phase transitions as a function of the measurement rate, depending on how much information about the quantum dynamics the eavesdropper has access to. For random unitary circuits with U(1) symmetry, we present an optimal classical classifier to reconstruct the global charge from local measurement outcomes only. We demonstrate the existence of phase transitions in the performance of this classifier in the thermodynamic limit. We also study numerically improved classifiers by including some knowledge about the unitary gates pattern.

DOI: 10.1103/PhysRevLett.129.200602

Introduction.—A recent breakthrough in our understanding of open quantum systems has been the discovery of measurement-induced phase transitions (MIPTs) in monitored quantum systems [1–4]. MIPTs have been best characterized in random quantum circuits, but seem to be a generic consequence of the competition between chaotic dynamics and measurements [1-54]. The best-studied MIPT, in random circuits, is a transition in the properties of a quantum state conditional on a set of measurement outcomes. It has multiple equivalent formulations, of which the most relevant one for our purposes is as follows [11]. When the measurement rate is high, local measurements can rapidly distinguish different initial states; in this "pure" phase, conditional on the outcomes, an initially mixed state quickly becomes pure. When the measurement rate is low, scrambling dominates, so initially distinct states become indistinguishable by local measurements. In this "mixed" phase, an initially mixed state remains mixed for times that scale exponentially with system size [11]. Mixed-phase dynamics forms a quantum error correcting code in the sense that it protects initial-state information from local observers [10,11,53]. Studying the MIPT as formulated above requires repeated generation of the same set of measurement outcomes, which in turn requires running each circuit a number of times that grows exponentially with system size and evolution time. Experimental studies of the MIPT have therefore been limited to very small systems [36,52].

In principle, the measurement outcomes in the pure phase suffice to distinguish any two initial states. Thus one would have a way around postselection if one could initialize the system in a mixed state, run the circuit once while recording the measurement outcomes, and use the outcomes to *predict* some property of the resulting pure

state that can be measured in a single shot. In the original random-circuit setting, this task is impractical, at least on a classical computer: to distinguish the two initial states, one would need to time evolve both with the specified measurement outcomes, and this is exponentially hard even with full knowledge of the unitary evolution operator and the measurement locations. (Similar challenges arise in the problem of reconstructing information from evaporating black holes [55–57].) Without such knowledge, predicting any local property of the final state is impossible: the space of possible unitaries involves arbitrary single-site rotations, so the knowledge gleaned from previous measurements is in a basis that is effectively hidden from the predictor.

Here, we show that constraining the unitary dynamics to have a single conserved charge (and measuring the local charge density) makes it possible to accurately predict an observable (namely, the total charge) on a single run of the circuit, even without knowledge of the gates. We consider a one-dimensional system of L qubits with a conserved U(1)charge $Q = \sum_i q_i$, where $q_i = (Z_i + 1)/2$. We initialize the system in one of two charge states $|Q_0\rangle$, or $|Q_1\rangle$. We then evolve the system in time with a brickwork of random unitaries, with each time step corresponding to two layers of gates acting on even and odd sites. The gates are chosen to conserve the U(1) charge, but are otherwise Haar random [58,59]. At each timestep, we allow an eavesdropper ("Eve") to measure the local charge q_i on each site of the system with independent probability p. At some time t_f that unless otherwise specified we will take to be $t_f = L$, Eve uses the measurement record and a decoding algorithm to produce a guess of the charge of the initial state (Fig. 1). Eve then shares her prediction and is told if it is correct. Symmetric

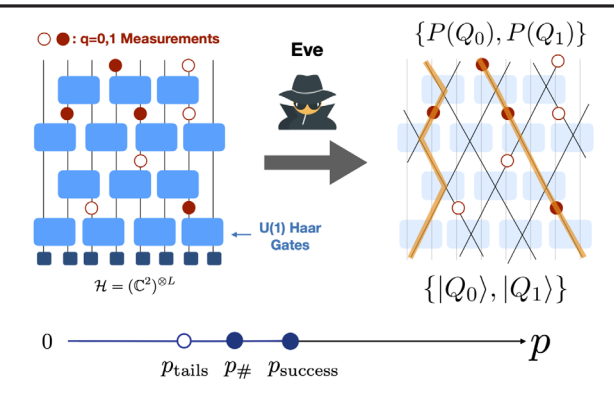


FIG. 1. Setup. An eavesdropper (Eve) attempts to reconstruct the global charge of a random quantum circuit from local charge measurements using a classical classifier. Eve can make exact predictions with success probability tending to 1 in the thermodynamic limit above the success transition $p_{\rm success}$. The success transition of the classifier is lower bounded by the charge sharpening transition $p_{\rm \#}$ of the system. At $p=p_{\rm tails}$, the distribution of the probability of correct label changes shape (see text). For the qubit model considered in this Letter $p_{\rm tails} \simeq p_{\rm \#}$, but including neutral degrees of freedom would increase $p_{\rm \#}$ towards $p_{\rm success}$ [42].

monitored quantum circuits exhibit a charge-sharpening transition at $p=p_{\#}$, within the mixed phase, that separates a phase where the final state conditional on the circuit and measurement outcomes has a definite charge from one where it does not [41,42]. In the case where Eve has unlimited resources, she can accurately predict the outcome if p exceeds $p_{\#}$ —the purification transition will play no role in the following.

Here, we argue that if Eve only has access to the measurement records, and has no knowledge about the unitary gates that were applied in each circuit except their distribution ("eavesdropping" scenario), the optimal decoding algorithm can be constructed by counting charge configurations consistent with the measurement outcomes the observer receives. This involves evaluating the partition sum of a classical statistical mechanics model, a task that can be efficiently performed on a classical computer. We also show that knowledge of the dynamics in between measurements can be used to improve the classifier ("learning" scenario), and discuss various transitions associated with this learning problem.

Independent measurements estimate.—For small measurement probability $p \ll 1$, it is natural to assume that the measurement outcomes $\{\vec{m}\}$ are independent. To estimate the charge, Eve can then simply use the averaged charge $Q_{\text{estimate}} = (L/M) \sum_{n=1}^{M} m_n$ with $M \sim 2 p t_f L$ the number of measurements, and determine whether it is closer to Q_0 or Q_1 . Assuming independent measurements and using the central limit theorem, the probability of success ("accuracy") of Eve to distinguish two charges $Q_0 = L/2$ and $Q_1 = L/2 - 1$ is

$$\alpha_{\text{lower bound}} = \frac{1}{2} \left(1 + \text{erf} \sqrt{\frac{pt_f}{L}} \right).$$
 (1)

In general, measurement outcomes are correlated in interesting ways that can be used to improve the charge estimate, and this uncorrelated result lower bounds the accuracy of other more effective classifiers.

Optimal classifier.—Charge conservation and locality induce correlations between measurement outcomes; accounting for these correlations allows us to outperform the independent-measurements estimate. For example, measuring three out of four legs of a gate determines the charge at the fourth, or measuring a charge q=1 in one of the incoming legs and q=0 in one of the outgoing legs fully determines the charges of the other two legs even if they are not measured.

The constraints from charge conservation can be turned into an efficient classifier. Intuitively, in the absence of information about the underlying physical dynamics, the best Eve can do is count charge configurations compatible with the measurement outcomes, assuming that charges perform random walks with the same diffusion constant as the quantum model. More formally, marginalizing over the gates U, the probability to observe the outcomes $\{m\}$ for a given charge Q is given by $P(\{m\}|Q) = \mathbb{E}_U P(\{m\}|U,Q)$. Eve can then use $P(Q|\{\vec{m}\}) = P(\{\vec{m}\}|Q)/[P(\{\vec{m}\}|Q_0) +$ $P(\{\vec{m}\}|Q_1)$ to determine which charge is more likely given a set of measurement outcomes $\{\vec{m}\}\$. Performing the average over U leads to an effective charge dynamics where at each time step, charges can either hop or remain at the same position with equal probability 1/2. This Markov process of hard-core random walks is known as the (discrete time) symmetric exclusion process (SEP) [60] subject to quenched constraints from measurements, which Eve could simulate efficiently on a classical computer. In the Supplemental Material [61], we show that this is indeed the optimal scheme, in the sense that it minimizes the misclassification probability. Remarkably, the same model also emerged in the context of measurement-induced charge-sharpening phase transitions in the limit of large onsite Hilbert space dimension [41,42].

To efficiently compute $P(\{m\}|Q)$, we use matrix-product state (MPS) methods, and represent this stochastic dynamics algebraically. The initial distribution over basis states in the Haar model is uniform over all states of a fixed charge Q. Represent this initial probability distribution of charge possibilities by a vector of size 2^L : $|\phi(0)| = |Q| = \binom{N}{Q}^{-1} \sum_{i:Q(i)=Q} |i|$, where we use the ket-like notation $|\psi|$ to denote a probability vector. The update to the probability distribution $|\phi(t)|$ due to the unitary at position i can be represented by the application of the transfer matrix (Markov operator) of the SEP

$$T_{i} = \begin{pmatrix} 1 & 0 & 0 & 0 \\ 0 & 1/2 & 1/2 & 0 \\ 0 & 1/2 & 1/2 & 0 \\ 0 & 0 & 0 & 1 \end{pmatrix}, \tag{2}$$

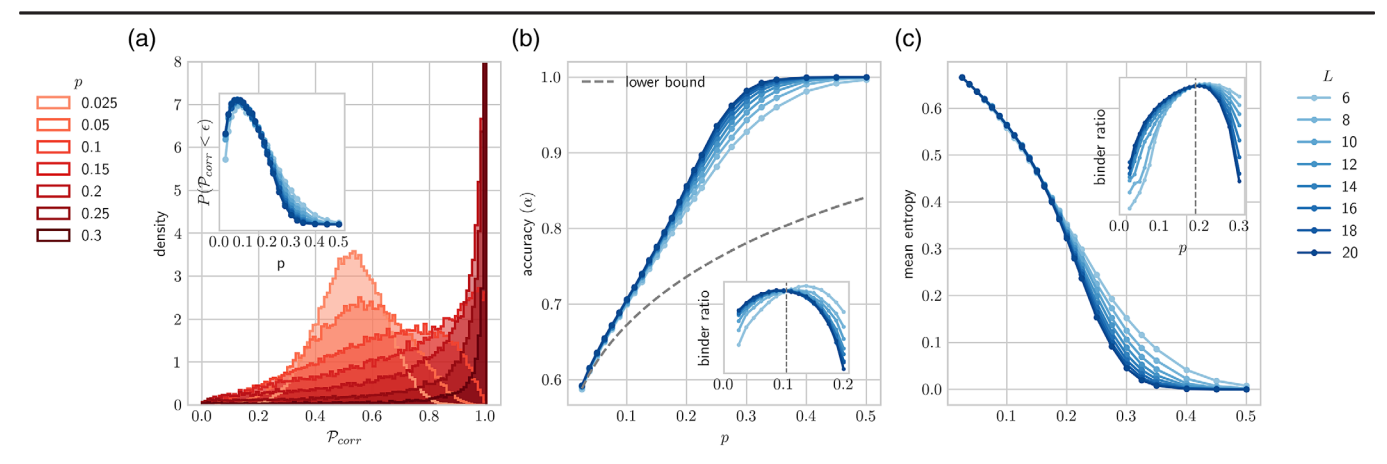


FIG. 2. Optimal classifier. (a) Probability distribution of the "probability associated with the correct charge label," $\mathcal{P}_{\text{corr}}$ for L=20. Inset: Weight in lower tail of distribution of $\mathcal{P}_{\text{corr}}$, $\epsilon=0.4$. The distribution changes through three distinct regimes: approximately Gaussian for $0 , power law for <math>p=p_{\text{tails}}$, exponential for $p>p_{\text{tails}}$. (b) Accuracy of the classifier. Inset: The Binder ratio shows a crossing at $p_{\text{tails}} \simeq 0.1$. (c) The mean entropy as an order parameter for the success transition, above which Eve can systematically make accurate predictions in the thermodynamic limit. Inset: the Binder ratio has a crossing at $p_{\text{success}} \simeq 0.2$.

to the probability distribution $|\phi(t)|$, written in the basis $\{00, 10, 01, 11\}$ for sites i, i+1. Every time the quantum state is measured at a site k, the corresponding probability vector $|\phi(t)|$ must be modified such that all states inconsistent with the measurement outcome on that site have probability 0. This can be achieved by applying the projector onto the correct measurement outcome. In applying the projector, the one-norm of the probability distribution decreases, by an amount corresponding to the fraction of trajectories that were inconsistent with that measurement outcome.

Define $T(\vec{m}_t)$ to be the linear operator that updates the probability vector from time t to t+1, given the constraints represented by the measurements. After time t_f , we have a state $|\phi(t_f)| = \prod_{t=1}^{t_f} T(\vec{m}_t)|Q|$ representing the uniform distribution over all charge trajectories that are consistent with both the measurement outcomes and the charge Q. The one-norm of the state represents the fraction of all possible trajectories of the charges in the Haar-random circuit that are compatible with the constraints—and can be found by the dot product of the probability vector with the (unnormalized) uniform distribution over all states $|1) = \sum_i |i|$,

$$P(\{\vec{m}\}|Q) = (1|\prod_{t=1}^{l_f} T(\vec{m}_t)|Q).$$
 (3)

Efficiency.—This probability can be found for a given circuit realization by explicitly evolving the state $|Q\rangle$ using a full representation of the probability vector. Naively, this algorithm scales as $\mathcal{O}(\operatorname{poly}(2^L))$. We can do better by noticing that the circuits and measurements (since they are not determined by properties of the time evolving state, but by the separate dynamics in the Haar circuit) represent a set of predetermined linear operations applied to the initial

state. Instead of applying them to the (highly entangled) state $|Q\rangle$, we can apply them in reverse to the (weakly entangled) state $|1\rangle$ as $(\psi(t_f)) = (1|\prod_{t=1}^{t_f} T(\vec{m}_t))$. Because of the nonunitary of the SEP dynamics, the entanglement growth generated by the transfer matrix is significantly lower than that in the Haar circuit, and so the system can be represented by an MPS with a bond dimension that grows sublinearly in time. This allows simulation of systems up to large sizes using MPS algorithms like TEBD [62,63].

The state $|Q\rangle$ cannot be efficiently represented on a classical computer, and so we cannot efficiently compute the dot product in Eq. (3). We can however, efficiently sample from $(\psi(t_f))$ (since it has a low bond dimension MPS representation) to produce an estimate of P(Q). We also note that this statistical mechanics problem has positive Boltzmann weights, and could be simulated efficiently using Monte Carlo methods.

Success transition.—In order to probe the performance of the classifier, we consider its performance on N=40,000 random Haar measurement records. While we generate this data using a classical computer and are thus limited to modest system sizes ($L\sim20$), we emphasize that our classifier can be run efficiently on measurement records generated by quantum processors on much larger systems. Half the records are generated from initial state $|Q_0\rangle=|L/2\rangle$, defined to be the uniform superposition over bitstrings at half filling, the other half from $|Q_1\rangle=|L/2-1\rangle$.

The task assigned the classifier is determining which state the record was generated from. Given the probabilities $P(Q_1|\{\vec{m}\})$, $P(Q_0|\{\vec{m}\})$ from the stat. mech. model, the classifier chooses the Q such that $P(Q|\{\vec{m}\})$ is maximal. The accuracy α of this classifier as a function of measurement rate and system size is presented in Fig. 2(b). The classifier gets better at solving the task as the measurement probability increases, as expected.

To get a better sense of the distribution of the classifier predictions across different measurement outcomes, we define the "probability of correct label" $\mathcal{P}_{\text{corr}}$ as follows. Suppose the initial state has charge Q^* (unknown to Eve). Eve begins with no information about the charge, then updates her probabilities based on the observed measurement outcomes. Her posterior probability for the correct charge label Q^* is denoted $\mathcal{P}_{\text{corr}}$: i.e., $\mathcal{P}_{\text{corr}} = P(Q^* | \{\vec{m}\})$. Note that since Eve is told the value of Q^* at the end of each run, $\mathcal{P}_{\text{corr}}$ is measurable for each run, so Eve has access to the entire probability distribution $P(\mathcal{P}_{\text{corr}})$, plotted in Fig. 2(a). In terms of $\mathcal{P}_{\text{corr}}$, the accuracy [Fig. 2(b)] is $P(\mathcal{P}_{\text{corr}} > 0.5)$.

The entropy of the binary distribution $\{P_{corr}, 1 - P_{corr}\}$ corresponds to the confidence of the classifier in its decision—irrespective of the ground truth label. The binder ratio [64] of the entropy has a crossing at $p_{\text{success}} \approx 0.2$, which corresponds to a "success transition." Above p_{success} , Eve can reconstruct the charge of the system exactly (i.e., with success probability tending to 1 as $L \to \infty$). Note that while Eve succeeds whenever $\mathcal{P}_{corr} > 1/2$, we need $\mathcal{P}_{corr} \rightarrow 1$ to guarantee that the measurement record uniquely identifies the charge. Interestingly, this success transition in the classifier also has an interpretation as a charge-sharpening transition in a charge-conserving model with large on-site Hilbert space [41], and its critical properties are Kosterlitz-Thouless-like [42]. In general, we have the constraint $p_{\#} \le p_{\text{success}}$, with $p_{\#} \simeq 0.09$ for qubit systems [41]: classifiers can only make systematic, exact predictions above the sharpening transition.

The full distribution of \mathcal{P}_{corr} [Fig. 2(a)] reveals a richer structure. For low $p < p_{tails} \simeq 0.1$, the measurement rate is insufficient for the observer to fix the charge, resulting is an approximately Gaussian distribution of \mathcal{P}_{corr} . Around $p = p_{tails}$, the tails of distribution of \mathcal{P}_{corr} empirically change from Gaussian to power-law like. This apparent transition in the tails of the distribution can also be detected from the Binder ratio [64] of \mathcal{P}_{corr} [inset of Fig. 2(b)], and from the power-law shape of the distribution of \mathcal{P}_{corr} , see inset of Fig. 2(a). Note that even though the quantity $1 - \mathbb{E}(\mathcal{P}_{corr})$ [where $\mathbb{E}(\dots)$ denotes an average] is itself an order parameter for the success transition [61], the heavy-tailed distribution allows its Binder ratio to cross at a measurement rate that is different from $p_{success}$. It would be interesting to analyze these tail transitions further in future work.

Biased classifier.—While the above classifier is optimal without additional knowledge about the circuit, it can be improved if Eve has some information about the underlying dynamics of the system (learning scenario). Let us assume now that for each run of the experiment, Eve receives the set of measurement outcomes and locations $\{\vec{m}, \vec{x}\}$, and the details of the unitary gates $\{U_{it}\}_{\forall i,t}$ that were applied to generate this measurement record.

There is a trivial, optimal, exponentially classically hard algorithm—the observer can run the circuit starting from

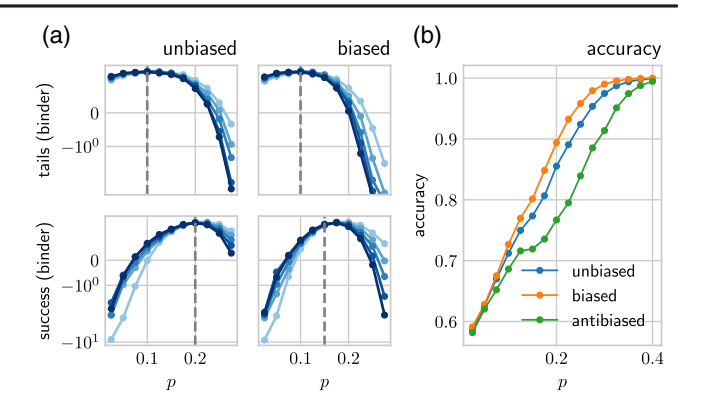


FIG. 3. Biased classifier. (a) The success transition is lowered by including information about the hopping probabilities in the classifier (biased model), while the accuracy transition remains unchanged. The color code is the same as in Fig. 2. (b) The classifier accuracy α is improved by including information about the hopping probabilities in the classifier.

 $|Q_0\rangle$, and $|Q_1\rangle$, measure the charge in the locations specified and count how many times the measurement record \vec{m} arises. We expect this algorithm to succeed above the charge-sharpening transition $(p>p_{\#})$. A more interesting task is to find an *efficient* classical algorithm that improves on the zero-knowledge classifier above. Define the hopping amplitude of a unitary $h(U)=|\langle 01|U|10\rangle|^2$. This has the properties $\overline{h(U)}=\frac{1}{2}$, where the overline indicates average over Haar, h(SWAP)=1 and $h(\mathbb{I})=0$. We can then modify the classifier above using the disordered hopping probabilities:

$$T_{i}(t) = \begin{pmatrix} 1 & 0 & 0 & 0 \\ 0 & p_{it} & 1 - p_{it} & 0 \\ 0 & 1 - p_{it} & p_{it} & 0 \\ 0 & 0 & 0 & 1 \end{pmatrix}$$
(4)

and three classifiers—unbiased, with $p_{it} = \frac{1}{2}$, biased, with $p_{it} = 1 - h(U_{it})$, and antibiased, with $p_{it} = h(U_{it})$. The unbiased model is the same as before, the biased model has hopping amplitudes that match the Haar-random circuit, and the antibiased model has hopping amplitudes that are opposite to the biased one. The performance of the biased classifier is summarized in Fig. 3. As expected, the biased model improves the accuracy of the classifier, although it does not change the location of the accuracy transition. The biased model has a lower success transition at $p_{\text{success}} \simeq 0.15$, closer to the fundamental sharpening bound $p_{\#} \simeq 0.09$. Additional results on the antibiased classifier are presented in the Supplemental Material [61].

Discussion.—When the measurement rate *p* is high enough, the history of measurement outcomes suffices to distinguish any two initial states, and quantum information in the system is unprotected from its environment. Even if the environment contains this "which-state" information,

extracting it and predicting the state of the system naively requires (a) full knowledge of the circuit, and (b) e^L resources for a chain of length L. We showed here that, for local dynamics with a conservation law, one can extract which-state information with polynomial overhead and with no knowledge of the gates in the circuit, by exploiting hydrodynamic correlations between measurements at different times. The threshold for in-practice extractability, p_{success} , exceeds that for in-principle extractability, $p_{\#}$. An interesting open question is whether, between these thresholds, the charge can be extracted given full knowledge of the circuit but only polynomial resources on a classical computer.

Our setup is analogous to the problem in black-hole physics where Alice drops a qubit into an old black hole and Bob attempts to reconstruct it from the emitted radiation [55]. The question addressed here is distinct (but in a sense "dual") to the problem of finding optimal decoders in the volume-law phase of the standard MIPT [10,11,53]. There, the measurement record contains no information about the encoded qubit, but is instead used to find a unitary operation *on the circuit* that unscrambles the input qubit. In our setup, the input qubit has leaked into the environment, and the task is instead to unscramble the environment. It would be interesting to extend our results to this decoding problem in symmetric circuits, and to explore consequences for covariant error correction [65,66].

We thank Kun Chen, Michael Gullans, David Huse, Jed Pixley, Justin Wilson, and Aidan Zabalo for useful discussions and collaborations on related projects, and Michael Gullans for helpful comments on this manuscript. We acknowledge support from the NSF through Grants No. DMR-1653271 (S. G.), No. DMR-1653007 (A. C. P.), the Air Force Office of Scientific Research under Grant No. FA9550-21-1-0123 (F. B. and R. V.), and the Alfred P. Sloan Foundation through Sloan Research Fellowships (A. C. P. and R. V.).

- [1] B. Skinner, J. Ruhman, and A. Nahum, Measurement-Induced Phase Transitions in the Dynamics of Entanglement, Phys. Rev. X 9, 031009 (2019).
- [2] Y. Li, X. Chen, and M. P. A. Fisher, Quantum Zeno effect and the many-body entanglement transition, Phys. Rev. B **98**, 205136 (2018).
- [3] A. Chan, R. M. Nandkishore, M. Pretko, and G. Smith, Unitary-projective entanglement dynamics, Phys. Rev. B 99, 224307 (2019).
- [4] A. C. Potter and R. Vasseur, Entanglement dynamics in hybrid quantum circuits, in *Entanglement in Spin Chain* (Springer Nature, Switzerland, 2022).
- [5] X. Cao, A. Tilloy, and A. D. Luca, Entanglement in a fermion chain under continuous monitoring, SciPost Phys. 7, 24 (2019).

- [6] M. Szyniszewski, A. Romito, and H. Schomerus, Entanglement transition from variable-strength weak measurements, Phys. Rev. B 100, 064204 (2019).
- [7] M. J. Gullans and D. A. Huse, Scalable Probes of Measurement-Induced Criticality, Phys. Rev. Lett. 125, 070606 (2020).
- [8] C.-M. Jian, Y.-Z. You, R. Vasseur, and A. W. W. Ludwig, Measurement-induced criticality in random quantum circuits, Phys. Rev. B 101, 104302 (2020).
- [9] Y. Bao, S. Choi, and E. Altman, Theory of the phase transition in random unitary circuits with measurements, Phys. Rev. B 101, 104301 (2020).
- [10] S. Choi, Y. Bao, X.-L. Qi, and E. Altman, Quantum Error Correction in Scrambling Dynamics and Measurement-Induced Phase Transition, Phys. Rev. Lett. 125, 030505 (2020).
- [11] M. J. Gullans and D. A. Huse, Dynamical Purification Phase Transition Induced by Quantum Measurements, Phys. Rev. X 10, 041020 (2020).
- [12] A. Zabalo, M. J. Gullans, J. H. Wilson, S. Gopalakrishnan, D. A. Huse, and J. H. Pixley, Critical properties of the measurement-induced transition in random quantum circuits, Phys. Rev. B 101, 060301 (2020).
- [13] N. Lang and H. P. Büchler, Entanglement transition in the projective transverse field Ising model, Phys. Rev. B 102, 094204 (2020).
- [14] S. Vijay, Measurement-driven phase transition within a volume-law entangled phase, arXiv:2005.03052.
- [15] O. Lunt and A. Pal, Measurement-induced entanglement transitions in many-body localized systems, Phys. Rev. Res. 2, 043072 (2020).
- [16] Q. Tang and W. Zhu, Measurement-induced phase transition: A case study in the nonintegrable model by density-matrix renormalization group calculations, Phys. Rev. Res. **2**, 013022 (2020).
- [17] X. Turkeshi, R. Fazio, and M. Dalmonte, Measurement-induced criticality in (2+1)-dimensional hybrid quantum circuits, Phys. Rev. B **102**, 014315 (2020).
- [18] Y. Fuji and Y. Ashida, Measurement-induced quantum criticality under continuous monitoring, Phys. Rev. B 102, 054302 (2020).
- [19] M. Szyniszewski, A. Romito, and H. Schomerus, Universality of Entanglement Transitions from Stroboscopic to Continuous Measurements, Phys. Rev. Lett. 125, 210602 (2020).
- [20] J. Iaconis, A. Lucas, and X. Chen, Measurement-induced phase transitions in quantum automaton circuits, Phys. Rev. B **102**, 224311 (2020).
- [21] B. Yoshida, Decoding the entanglement structure of monitored quantum circuits, arXiv:2109.08691.
- [22] A. Lavasani, Y. Alavirad, and M. Barkeshli, Measurement-induced topological entanglement transitions in symmetric random quantum circuits, Nat. Phys. **17**, 342 (2021).
- [23] X. Turkeshi, A. Biella, R. Fazio, M. Dalmonte, and M. Schiró, Measurement-induced entanglement transitions in the quantum Ising chain: From infinite to zero clicks, Phys. Rev. B 103, 224210 (2021).
- [24] S. Sang, Y. Li, T. Zhou, X. Chen, T. H. Hsieh, and M. P. Fisher, Entanglement negativity at measurement-induced criticality, PRX Quantum 2, 030313 (2021).

- [25] Y. Li and M. P. A. Fisher, Robust decoding in monitored dynamics of open quantum systems with Z_2 symmetry arxiv.2108.04274.
- [26] S. Sang and T. H. Hsieh, Measurement-protected quantum phases, Phys. Rev. Res. **3**, 023200 (2021).
- [27] Y. Li, X. Chen, A. W. W. Ludwig, and M. P. A. Fisher, Conformal invariance and quantum nonlocality in critical hybrid circuits, Phys. Rev. B **104**, 104305 (2021).
- [28] Y. Li, S. Vijay, and M. P. A. Fisher, Entanglement domain walls in monitored quantum circuits and the directed polymer in a random environment, arxiv.2105.13352.
- [29] M. J. Gullans, S. Krastanov, D. A. Huse, L. Jiang, and S. T. Flammia, Quantum Coding with Low-Depth Random Circuits, Phys. Rev. X 11, 031066 (2021).
- [30] M. Ippoliti, M. J. Gullans, S. Gopalakrishnan, D. A. Huse, and V. Khemani, Entanglement Phase Transitions in Measurement-Only Dynamics, Phys. Rev. X 11, 011030 (2021).
- [31] R. Fan, S. Vijay, A. Vishwanath, and Y.-Z. You, Self-organized error correction in random unitary circuits with measurement, Phys. Rev. B 103, 174309 (2021).
- [32] Y. Bao, S. Choi, and E. Altman, Symmetry enriched phases of quantum circuits, Ann. Phys. (Amsterdam) 435, 168618 (2021), special issue on Philip W. Anderson.
- [33] O. Alberton, M. Buchhold, and S. Diehl, Entanglement Transition in a Monitored Free-Fermion Chain: From Extended Criticality to Area Law, Phys. Rev. Lett. **126**, 170602 (2021).
- [34] O. Lunt, M. Szyniszewski, and A. Pal, Measurementinduced criticality and entanglement clusters: A study of one-dimensional and two-dimensional clifford circuits, Phys. Rev. B 104, 155111 (2021).
- [35] A. Lavasani, Y. Alavirad, and M. Barkeshli, Topological Order and Criticality in (2+1)D Monitored Random Quantum Circuits, Phys. Rev. Lett. **127**, 235701 (2021).
- [36] C. Noel, P. Niroula, D. Zhu, A. Risinger, L. Egan, D. Biswas, M. Cetina, A. V. Gorshkov, M. J. Gullans, D. A. Huse, and C. Monroe, Observation of measurement-induced quantum phases in a trapped-ion quantum computer, Nat. Phys. 18, 760 (2022).
- [37] M. Van Regemortel, Z.-P. Cian, A. Seif, H. Dehghani, and M. Hafezi, Entanglement Entropy Scaling Transition Under Competing Monitoring Protocols, Phys. Rev. Lett. 126, 123604 (2021).
- [38] A. Nahum, S. Roy, B. Skinner, and J. Ruhman, Measurement and entanglement phase transitions in all-to-all quantum circuits, on quantum trees, and in Landau-Ginsburg theory, PRX Quantum 2, 010352 (2021).
- [39] G. S. Bentsen, S. Sahu, and B. Swingle, Measurementinduced purification in large-n hybrid Brownian circuits, Phys. Rev. B 104, 094304 (2021).
- [40] S.-K. Jian and B. Swingle, Phase transition in von Neumann entanglement entropy from replica symmetry breaking, arXiv:2108.11973.
- [41] U. Agrawal, A. Zabalo, K. Chen, J. H. Wilson, A. C. Potter, J. H. Pixley, S. Gopalakrishnan, and R. Vasseur, Entanglement and charge-sharpening transitions in U(1) symmetric monitored quantum circuits, arXiv:2107.10279.
- [42] F. Barratt, U. Agrawal, S. Gopalakrishnan, D. A. Huse, R. Vasseur, and A. C. Potter, Field Theory of Charge

- Sharpening in Symmetric Monitored Quantum Circuits, Phys. Rev. Lett. **129**, 120604 (2022).
- [43] Y. Li, R. Vasseur, M. P. A. Fisher, and A. W. W. Ludwig, Statistical mechanics model for Clifford random tensor networks and monitored quantum circuits, arXiv: 2110.02988.
- [44] S. Czischek, G. Torlai, S. Ray, R. Islam, and R. G. Melko, Simulating a measurement-induced phase transition for trapped-ion circuits, Phys. Rev. A 104, 062405 (2021).
- [45] Z. Weinstein, Y. Bao, and E. Altman, Measurement-Induced Power Law Negativity in an Open Monitored Quantum Circuit, Phys. Rev. Lett. **129**, 080501 (2022).
- [46] P. Sierant, G. Chiriacò, F. M. Surace, S. Sharma, X. Turkeshi, M. Dalmonte, R. Fazio, and G. Pagano, Dissipative floquet dynamics: From steady state to measurement induced criticality in trapped-ion chains, Quantum 6, 638 (2022).
- [47] Y. Han and X. Chen, Measurement-induced criticality in F_2 -symmetric quantum automaton circuits, Phys. Rev. B **105**, 064306 (2022).
- [48] Y. Bao, M. Block, and E. Altman, Finite time teleportation phase transition in random quantum circuits, arXiv: 2110.06963.
- [49] A. Zabalo, M. J. Gullans, J. H. Wilson, R. Vasseur, A. W. W. Ludwig, S. Gopalakrishnan, D. A. Huse, and J. H. Pixley, Operator Scaling Dimensions and Multifractality at Measurement-Induced Transitions, Phys. Rev. Lett. 128, 050602 (2022).
- [50] S. Sahu, S.-K. Jian, G. Bentsen, and B. Swingle, Entanglement phases in large-n hybrid Brownian circuits with long-range couplings, arXiv:2109.00013.
- [51] P. Sierant and X. Turkeshi, Universal Behavior Beyond Multifractality of Wave Functions at Measurement-Induced Phase Transitions, Phys. Rev. Lett. 128, 130605 (2022).
- [52] J. M. Koh, S.-N. Sun, M. Motta, and A. J. Minnich, Experimental realization of a measurement-induced entanglement phase transition on a superconducting quantum processor, arXiv:2203.04338.
- [53] H. Dehghani, A. Lavasani, M. Hafezi, and M. J. Gullans, Neural-network decoders for measurement induced phase transitions, arXiv:2204.10904.
- [54] A. Zabalo, J. H. Wilson, M. J. Gullans, R. Vasseur, S. Gopalakrishnan, D. A. Huse, and J. H. Pixley, Infinite-randomness criticality in monitored quantum dynamics with static disorder, arXiv:2205.14002.
- [55] P. Hayden and J. Preskill, Black holes as mirrors: Quantum information in random subsystems, J. High Energy Phys. 09 (2007) 120.
- [56] D. Harlow and P. Hayden, Quantum computation vs. firewalls, J. High Energy Phys. 06 (2013) 085.
- [57] B. Yoshida and A. Kitaev, Efficient decoding for the Hayden-Preskill protocol, arXiv:1710.03363.
- [58] V. Khemani, A. Vishwanath, and D. A. Huse, Operator Spreading and the Emergence of Dissipative Hydrodynamics Under Unitary Evolution with Conservation laws, Phys. Rev. X 8, 031057 (2018).
- [59] T. Rakovszky, F. Pollmann, and C. W. von Keyserlingk, Diffusive Hydrodynamics of Out-of-Time-Ordered Correlators with Charge Conservation, Phys. Rev. X 8, 031058 (2018).

- [60] F. Spitzer, Interaction of Markov processes, Adv. Math. 5, 246 (1970).
- [61] See Supplemental Material at http://link.aps.org/supplemental/10.1103/PhysRevLett.129.200602 for a proof of the optimality of the stat. mec. decoder, and for additional data and variants of the learning problem.
- [62] G. Vidal, Efficient Classical Simulation of Slightly Entangled Quantum Computations, Phys. Rev. Lett. 91, 147902 (2003).
- [63] U. Schollwöck, The density-matrix renormalization group in the age of matrix product states, Ann. Phys. (Amsterdam) **326**, 96 (2011), january 2011 Special Issue.
- [64] K. Binder and D. W. Heermann, Theoretical foundations of the Monte Carlo method and its applications in statistical physics, in *Monte Carlo Simulation in Statistical Physics* (Springer, New York, 2010), pp. 5–67.
- [65] P. Faist, S. Nezami, V. V. Albert, G. Salton, F. Pastawski, P. Hayden, and J. Preskill, Continuous Symmetries and Approximate Quantum Error Correction, Phys. Rev. X 10, 041018 (2020).
- [66] L. Kong and Z.-W. Liu, Near-optimal covariant quantum error-correcting codes from random unitaries with symmetries, PRX Quantum 3, 020314 (2022).